TURBULENT FLAME MODELS FOR PREDICTION OF PRESSURE OSCILLATIONS IN GAS TURBINE BURNERS

Dmytro Iurashev
Università degli Studi di Genova, DICCA, via Montallegro 1, 16145 Genova, Italy
email: dmytro.iurashev@edu.unige.it

Giovanni Campa, Vyacheslav Anisimov, Andrea Di Vita, Ezio Cosatto, Federico Daccà
Ansaldo Energia S.p.A., PDE/ISV/TMC/TFC, via N. Lorenzi 8, 16152 Genova, Italy

Alp Albayrak
Professur für Thermofluiddynamik, TUM, Boltzmannstr. 15, D-85748 Garching, Germany

Humming is a dangerous, combustion-driven acoustic oscillation in gas-turbine burners, which may cause catastrophic damages, thus undermining manufacturers' competitiveness. Therefore those systems require humming prevention, which, in turn, requires predictive tools which are both reliable and fast. As a matter of principle, both perturbations of stoichiometry and flame velocity affect heat release. Moreover, the mentioned perturbations also lead to fluctuations in flame surface area, which should be accounted for in the modeling stage. Therefore, the thermo-acoustic model described in this work considers a combustion model, which relies on the propagation of the regress variable. Simulations are carried out by means of OpenFOAM environment. Modeling of heat release includes nonlinearities. The model solves non-linearized averaged Navier-Stokes equations for compressible fluids. Thus, it includes both convection and sound propagation. The scope of the work is to verify the sensitivity of the heat release model to velocity fluctuations on the BRS (Beschaufelter RingSpalt) burner test-rig at the Technische Universität München. Two flame models are used: the Turbulent Flame Closure (TFC) model and the Flame Speed Closure (FSC) one. However, both of them predict the distribution of the heat release shifted closer to the exit of the burner. Thus, the phase of the flame heat response to acoustic perturbations is lower than the experimentally obtained values. Further evolution of humming amplitudes could be observed in the time domain.

1. Introduction

In order to meet environment requirements gas turbine producers have to make their machines run in the lean combustion regime. However, in this regime gas turbines are prone to the so-called combustion instabilities. Usually the last refer to the high-amplitude pressure oscillations caused by interaction of acoustic, flame and stoichiometry. Such oscillations are able to cause excessive structural vibrations, fatigue and sometimes even catastrofic damage to combustion hardware. That is why there is an urgent need to understand the physical processes that are responsible so that methods to predict and prevent these instabilities should be developed.

There are several approaches to predict combustion instabilities [1]. One approach consists on the use of low order models, in which the combustor system is divided into series of simpler subsystems and mathematical transfer function matrices are used to connect lumped acoustic elements to each other. Another approach is to perform Large Eddy Simulations (LES) to model directly interaction between combustion, acoustics and flow. For specific configurations the use of LES is still computationally expensive. Alternative is to perform simulation using Helmholtz solver and a model for a Flame Transfer Function (FTF), whose parameters are extracted from acoustically forced LES or Unsteady Reynolds Averaged Navier Stokes (URANS) [2].

The described approaches usually refer to the frequency domain, but it was shown [3] that the operator that describes thermoacoustic system is non-normal. Thus, simulations ought to be done in time domain, in order to take into account possible transient growth of acoustic energy with further triggering nonlinearities and exchange of energy between modes [4]. Moreover, simulations in time domain permit us to predict amplitude of pressure oscillations, that is of high importance for the gas turbine producer.

In a previous work of ours [5] it was shown that the approach described in that work is able to predict limit cycle pressure oscillations. Description of the heat release is the core of that model. Thus, its choice is crucial for the correct simulation of the occurrence of combustion instabilities First the formula for the turbulent flame velocity proposed by Zimont et al. [6] has been introduced in the existing model [5]. Later, the heat release response to the the velocity fluctuations, the changes of the flame area [7] and the changes in flame position have been introduced. This was done resolving propagation of regress variable with the help of OpenFOAM based-in solver XiFoam. The swirl type BRS burner test rig from TUM [8] has been used for validating the proposed flame model.

2. Mathematical model

The combustion phenomena occurring in the test rig has been simulated through URANS [9], in which Favre averaging is used. The flow is assumed to be compressible. $k-\omega\ SST$ model of turbulence is used [10] because it resolves well both turbulence in the near-boundary zone and in the free-stream.

2.1 Features of OpenFOAM solver XiFoam

OpenFOAM solver XiFoam is a solver for compressible premixed/partially-premixed combustion with turbulence modeling [11]. For the simulations of combustion of homogeneous mixture of fuel and oxidant, it uses compressible PIMPLE (merged PISO-SIMPLE) algorithm in which, additionally to solving for the propagation of the enthalpy (Eq. (1)), also solves for the propagation of the enthalpy of unburnt gas (Eq. (2)):

$$\frac{\partial \rho h}{\partial t} + \nabla \cdot (\rho \mathbf{U} h) + \frac{\partial \rho K}{\partial t} + \nabla \cdot (\rho \mathbf{U} K) - \frac{\partial p}{\partial t} - \nabla \cdot (\rho D_t \nabla h) = 0, \tag{1}$$

$$\frac{\partial \rho h_u}{\partial t} + \nabla \cdot (\rho \mathbf{U} h_u) + \left[\frac{\partial \rho K}{\partial t} + \nabla \cdot (\rho \mathbf{U} K) - \frac{\partial p}{\partial t}\right] \frac{\rho}{\rho_u} - \nabla \cdot (\rho D_t \nabla h_u) = 0, \tag{2}$$

where ρ is the density of the air-fuel mixture, h is the enthalpy, h_u is the enthalpy of unburnt gas, t is the time, $\mathbf{U}$ is the vector of the mean velocity, K is the kinetic energy $K = |\mathbf{U}|^2/2$, p is the pressure, ρ_u is the density of unburnt mixture, D_t is the coefficient of turbulent diffusion.

Initial distribution of the enthalpy and the enthalpy of unburnt gases is taken from the initial fields of temperature and from the temperature of unburnt gases. The temperature and the temperature of unburnt gases are calculated from the respective enthalpies. Then, thermo-physical properties, such as density and heat diffusivity, are calculated from the respective temperatures. The laminar flame speed is calculated depending on the temperature of unburnt gases.

Moreover, XiFoam solves the transport equation for the regress variable b. In order to describe the propagation of the flame, first the TFC model proposed by Zimont et al. [6] was implemented into XiFoam. This model has been already used for BRS burner test rig [8]. Then, the FSC model proposed by Lipatnikov and Chomiak [12] was implemented in the solver. The results obtained from the two models are compared in this work.

2.2 Turbulent Flame Closure Model

In the TFC combustion model proposed by Zimont et al. [6], the flame front propagation is modeled by solving a transport equation (3) for the regress variable b.

$$\frac{\partial \rho b}{\partial t} + \nabla \cdot (\rho \mathbf{U} b) - \nabla \cdot (\rho D_t \nabla b) = -\rho_u S_t |\nabla b|, \tag{3}$$

where S_t is the turbulent flame speed, calculated as Eq. (5).

The regress variable is defined as the normalised fuel mass fraction. It is equal to 1 in the zone of unburnt gas and to 0 in the zone of burnt gas and is defined as

$$b = \frac{T_b - T}{T_b - T_u}, \tag{4}$$

where T_b is the temperature of the burnt gas, T is the temperature of gas at the current point and T_u is the temperature of the unburnt gas.

The turbulent flame speed in the TFC model is calculated as

$$S_t = A(u')^{0.75} S_{L,0}^{0.5} \alpha_u^{-0.25} l_t^{0.25}, \tag{5}$$

where A is model dimensionless constant taken to be equal to 0.52, u' is the velocity perturbation, $S_{L,0}$ is the unperturbed laminar flame speed, α_u is the thermal diffusivity of the unburnt mixture, l_t is the turbulence length scale that is calculated as

$$l_t = C_D \frac{(u')^3}{\epsilon}, \tag{6}$$

where C_D is the model dimensionless constant, ϵ is the turbulence dissipation rate.

2.3 Flame Speed Closure Model

The FSC model was proposed by Lipatnikov and Chomiak [12]. This model describes propagation of the flame in the limit case of absence of turbulence as well as in the case of fully developed turbulence (Eq. 7). Moreover, it takes into account dependence of diffusivity and turbulent flame speed on the time of flow propagation from the flame holder.

$$\frac{\partial \rho b}{\partial t} + \nabla \cdot (\rho \mathbf{U} b) - \nabla \cdot [\rho(\kappa + D_{t,t}) \nabla b] = -\frac{S_{L,0}^2}{4(\kappa + D_{t,t})} \rho_u (1-b) b - \rho_u S_{t,t} |\nabla b|, \tag{7}$$

where k is the molecular diffusivity. $D_{t,t}$ is the time-dependent coefficient of turbulent diffusion that is calculated as

$$D_{t,t} = D_t \left[1 - \exp\left(-\frac{t_{fd}}{\tau'} \right) \right]. \tag{8}$$

In Eq. 8 the flame development time t_{fd} is calculated as

$$t_{fd} = \frac{x - x_{flame\ holder}}{u_{mean}}, \tag{9}$$

where x is the current axial position, $x_{flame\ holder}$ is the axial position of the flame holder, u_{mean} is the axial mean gas flow velocity at the exit of the burner. τ' in Eq. 8 is the Lagrangian time scale of turbulence, calculated as $\tau' = D_t/u'^2$.

$S_{t,t}$ in Eq. 8 is the time-dependent turbulent flame velocity that is calculated as

$$S_{t,t} = S_t \left\{ 1 + \frac{\tau'}{t_{fd}} \left[\exp\left(-\frac{t_{fd}}{\tau'} \right) - 1 \right] \right\}^{0.5}, \tag{10}$$

where S_t is calculated using Eq. (5).

The first term on the right hand side of Eq. (7) takes into account the laminar flame speed in the limit case of $u' \rightarrow 0$ as well as additional term on the left hand side of this equation takes into account molecular diffusivity in the limit case of absence of turbulence. Using $D_{t,t}$ instead of D_t takes into account well-established time-dependance of turbulent diffusivity, as well as using $S_{t,t}$ instead of S_t makes the same for the turbulent flame speed [12].

2.4 Flame Transfer Function

The dynamic response of a flame to a flow perturbation can be represented in the frequency domain by its flame transfer function FTF(ω) (also "frequency response"). It relates fluctuations of mass flow rate or velocity u'_r at a reference position r upstream of the flame to fluctuations of the flame heat release $\dot{Q}'$:

$$FTF(\omega) = \frac{\dot{Q}'(\omega)/\bar{\dot{Q}}}{u'_r(\omega)/\bar{u}_r} \tag{11}$$

Here fluctuations $\dot{Q}'$ and u'_r are normalized with the respective mean values of heat release $\bar{\dot{Q}}$ and velocity $\bar{u}_r$. In experiments the flame transfer function FTF(ω) is computed from time series of fluctuations u'_r and $\dot{Q}'$ with spectral analysis applying harmonic excitation with a loudspeaker or siren at the inlet. In simulations advanced methods based on System Identification (SI) are used. More detailed procedure of obtaining FTF can be found in [8, 13].

3. Description of the BRS burner test-rig

The BRS test rig is "perfectly premixed" burner with an axial swirl generator mounted on a central bluff body (see Fig. 1). The burner exit is represented by an annular section with an inner diameter 16 mm and an outer diameter 40 mm. Swirl generator 30 mm length is positioned at 30 mm upstream of the burner exit. Combustion chamber has quadratic cross section of 90x90 mm. During the experiments the length of combustion chamber was 300 mm. However, for simulations the combustor length of 200 mm is used, because the heat release zone lays in the first 100 mm of the combustion chamber. Thus, the length taken into account is enough to simulate the behavior of the flame. In measurements perforated plated is mounted at the end of the combustion chamber making the outlet of combustion chamber non-reflecting. The fuel-air mixture is homogeneous with equivalence ratio of 0.77. Since the structure of the set-up is periodical, it can be represent by just one quarter of the test rig in our simulations. More details about experimental set-up can be found in [13]. Boundary conditions are the same as in [8], but with reflecting boundary condition at the inlet instead of non-reflecting. They are listed in table 1. For non-reflecting outlet boundary condition $waveTransmissive$ boundary condition is used [11].

4. Results

In Fig. 2a mean axial velocity in combustor middle cross plane obtained numerically with the FSC model is shown. From this figure it can be seen that the flow has maximum of the axial velocity

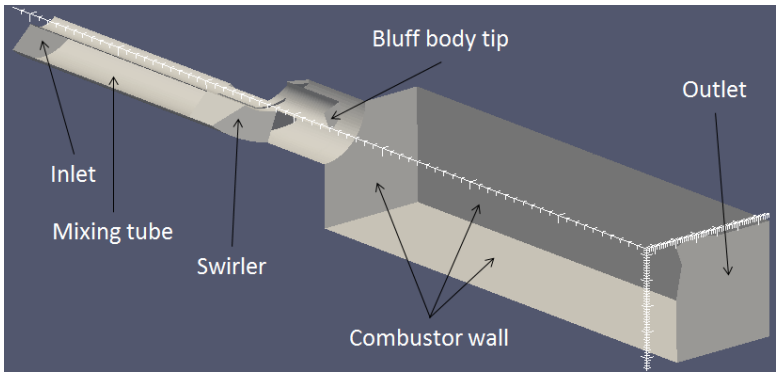

Figure 1: Scheme of the numerical set-up of the BRS test rig

Table 1: Boundary Conditions for the BRS numerical model [8]

Face	Boundary condition	Value
Inlet	Fixed velocity	$U = 11.3m/s$
Outlet	Non-reflective pressure outlet	$p = 101325Pa$
Mixing tube, swirler	Adiabatic no-slip wall	–
Combustor wall	Isothermal no-slip wall	$T = 600K$
Bluff body tip	Isothermal no-slip wall	$T = 600K$

between the flame holder and the heat release zone. Recirculation zones are in the middle of the chamber and near the outer corners close to the exit of the burner. In Fig. 2b normalized heat release obtained numerically with the FSC model is shown. From the figure it can be seen that the flame is attached to the flame holder.

As soon as authors of the FSC model are stressing that parameters C_D and Sc_t are not defined and can change from case to case [14], we have performed parametric analyses in order to fit experimental data. We have adjusted parameters C_D, Sc_t and u_{mean} in the FSC model. Changing value of C_D in the range from 0.16 to 0.7, turbulent flame velocity is decreased on 16% and is increased on 24%, respectively, in comparison with the default value of $C_D = 0.3$. Thus, the flame is expected to be significantly longer and shorter respectively. We took the value of turbulent Schmidt number Sc_t of 0.7, as it is commonly used in Computational Fluid Dynamics papers [14]. The value of u_{mean} initially is taken the same as at the inlet of the mixing tube, $11.3\ m/s$.

Results of the simulations are presented in Fig. 3a. In this figure distribution of area normalized intensity of the flame OH-Chemiluminescence measured in experiments is shown. Also area normalized heat release distributions along the axis of the burner using the FSC models are shown.

Despite significant changes in the value of the parameter C_D, no significant changes in the distribution of the heat release can be observed. Thus, the default value of $C_D = 0.3$ can be taken for further simulations.

Previous simulations showed that axial component of velocity between the flame holder and the heat release zone is about $18\ m/s$, much larger than the one taken before, $11.3\ m/s$ (Fig. 2a). Thus, $u_{mean} = 18\ m/s$ has been introduced in the model. Fig. 3a shows resulting area normalized heat release distribution obtained from the simulation. Having increased the value of u_{mean} on 60%, no notable changes in the position of the flame are observed. Hence, influence of this parameter on the $S_{t,t}$ (Eq. (10)) is not significant. The same can be said about the influence of the parameter Sc_t on the heat release distribution. In Fig. 3b the area normalized heat release distribution is shown for different values of Schmidt number $Sc_t = 0.3$ and $Sc_t = 0.7$ with $C_D = 0.3$, $u_{mean} = 18\ m/s$.

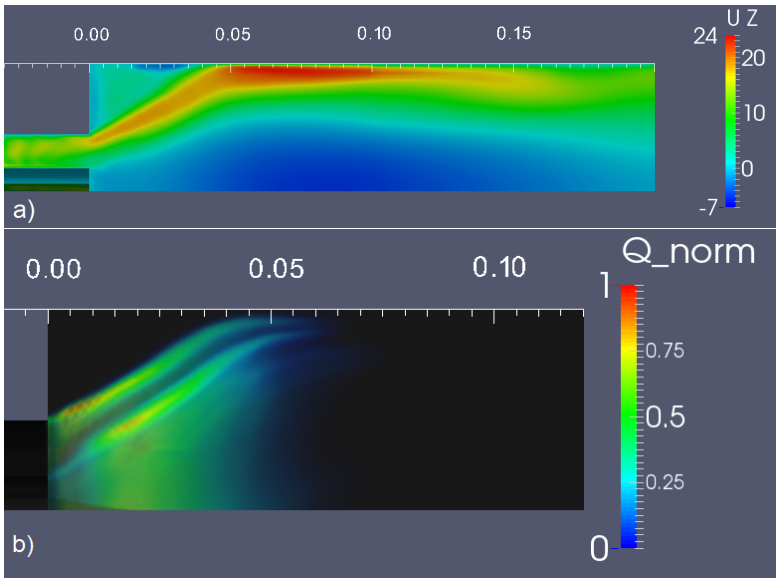

Figure 2: Axial velocity and normalized spatial distribution of the heat release obtained numerically using the FSC model with $C_D = 0.3$, $Sc_t = 0.7$, $u_{mean} = 18\ m/s$

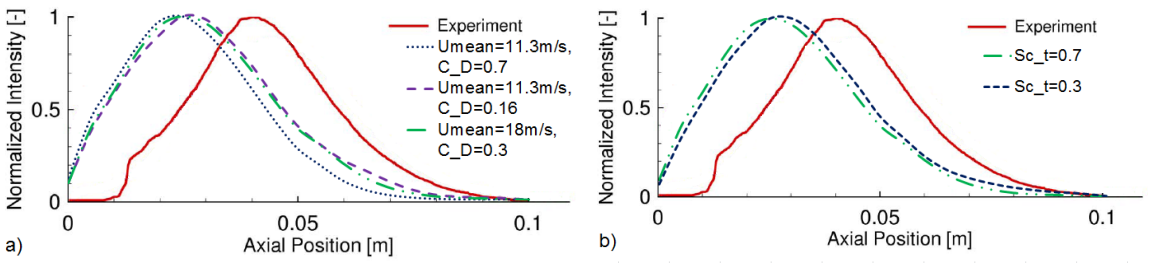

Figure 3: Area normalized flame intensity of the flame from experiments and are normalized heat release from simulations over the axis of the combustion chamber: a) simulations done using the FSC model with $Sc_t = 0.7$ and varying values of C_D and u_{mean}; b) simulations done with the FSC model and $C_D = 0.3$, $u_{mean} = 18\ m/s$ and varying values of Sc_t

For the simulations using TFC model values of parameters $C_D = 0.3$ and $Sc_t = 0.7$ are taken as suggested by [14]. As shown in Fig. 4, values of the heat release close to the exit from the burner is twice lower for the FSC model than for the TFC one. This difference is not very notable. Similar difference was noticed by the authors of the FSC model in the case of fully-developed turbulence [14]. It implies that turbulence of the flow at the exit of the burner is not as well-developed as in the far-field from the burner exit. That is why turbulent flame speed just at the exit of the burner must be much lower [12].

Despite the difference, both TFC and FSC models predict position of the flame incorrectly. Incorrect distribution of the heat release could be explained by the fact that in experiments walls of the chamber are made of glass and are not insulated. Thus, a heat flux is leaving combustion chamber in experiments through convective and radiative losses. Both TFC and FSC models are developed for adiabatic flames. These models in the way they are implemented in XiFoam are not able to predict correct position of the flame as the one described in this work. Their implementation in the current work is such that heat losses should be taken into account by the enthalpy of unburnt gas h_u. In the results presented in this paper temperature of unburnt gas T_u is set constant in the volume. Moreover, Eq. (2) is not solved because boundary conditions for T_u are not known and in the Eq. (2) there is no term that takes into account heat losses due to the radiation.

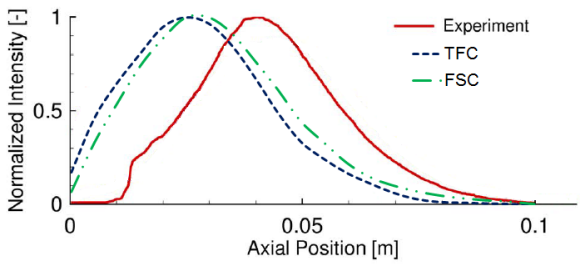

Figure 4: Area normalized flame intensity of the flame from experiments and are normalized heat release from simulations over the axis of the combustion chamber. Simulations done using the TFC model with $C_D = 0.3$, $Sc_t = 0.7$ and using the FSC model with $C_D = 0.3$, $Sc_t = 0.3$, $u_{mean} = 18\,m/s$

However, in combustion chambers of gas turbine engines we usually deal with almost completely adiabatic flames. As a consequence, in the future development of the approach described in [5] FSC model will be used to describe the flame propagation.

The simulations were excited at the inlet by perturbations on the characteristic ingoing wave with a broadband frequency-limited (1 kHz) discrete random binary signal and an amplitude of 10% of the mean inlet velocity. Reference plane for velocity measurement is situated at 0.005 m upstream the exit from the burner. In Fig. (5) the FTFs from experiments and SI are presented. Both of them present amplitudes with a local maximum in gain above unity, followed by a decrease at higher frequencies. Good agreement is found between experiments and simulations in amplitude for all range of frequencies. The phase from simulations is smaller in absolute value than the one from experiments, because the flame stabilizes in both shear layers, creating a shorter flame and reducing the timelag responses of the flame to the different perturbations. The phase error from simulations increases with frequency, increasing the discrepancies with respect to the experimental FTF.

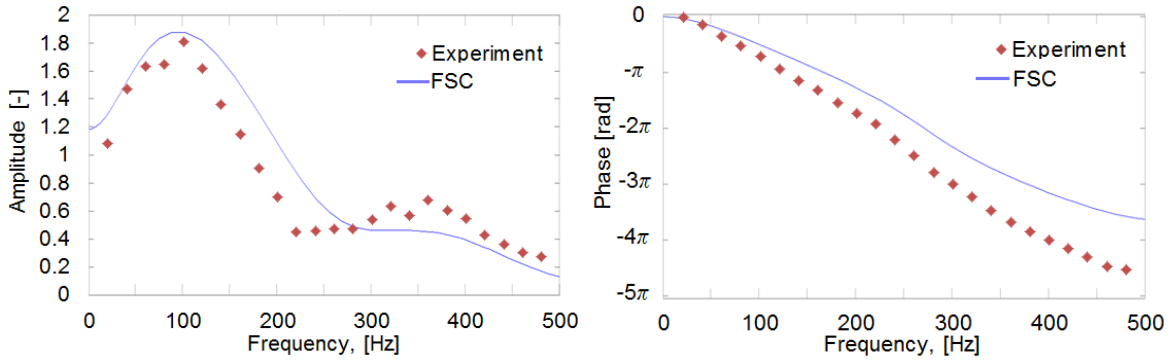

Figure 5: Flame transfer function from experiments and the one obtained using the FSC model

5. Conclusions

In this work we have applied the Turbulent Flame Closure and the Flame Speed Closure models to the BRS burner test rig. In simulations the heat release distribution is shifted towards the exit of the burner with respect to the one measured in the experiments. It is explained by the fact that both of these models are developed for adiabatic flames, and the flame under consideration is not fully adiabatic.

The distribution of amplitudes of the FTF predicted by simulations fits well experimental data.

The difference of phase distributions of FTF between simulations and experiments is explained by the shifted position of the flame.

In the future, the outcomes from the current paper will be merged with the outcomes from [5] to perform thermo-acoustic simulations of an industrial gas turbine burner.

6. Acknowledgements

This work is part of the Marie Curie Initial Training Network Thermo-acoustic and aero-acoustic nonlinearities in green combustors with orifice structures (TANGO). We gratefully acknowledge the financial support from the European Commission under call FP7-PEOPLE-ITN-2012.

REFERENCES

1. Lieuwen, T., *Unsteady Combustor Physics*, Cambridge University Press, Cambridge, UK, (2012).

2. Wolf, P., Staffelbach, G., Gicquel, L., Müller, J.-D., and Poinsot, T., Acoustic and large eddy simulation studies of azimuthal modes in annular combustion chambers, *Comb. and Flame*, **159** (11), pp. 3398–3413, (2012).

3. Wieczorek, K., Sensiau, C., Polifke, W., and Nicoud, F. Assessing non-normal effects in thermoacoustic systems with mean flow, *Physics of Fluids*, **23** (10), 107103, (2011).

4. Balasubramanian, K., Sujith, R. I. Non-normality and nonlinearity in combustion-acoustic interaction in diffusion flames, *J. Fluid Mech.*, **594**, 29–57 (2008).

5. Iurashev, D., Di Vita, A., Cosatto, E., Campa, G., Daccà, F., Bottaro, A. A Limit Cycle for Pressure Oscillations in a Gas Turbine Burner, *Proceedings of the 21st International Congress on Sound and Vibration*, Beijing, China, 13–17 July, (2014).

6. Zimont, V., Polifke, W., Bettelini, M. and Weisenstein. W. An Efficient Computational Model for Premixed Turbulent Combustion at High Reynolds Numbers Based on a Turbulent Flame Speed Closure, *J. of Gas Turbines Power*, **120**, 526-532, (1998).

7. Albayrak, A., Ulhaq, A., Blumenthal, R.S. and Polifke, W. Analytical Derivation of Laminar Premixed Flame Impulse Response to Equivalence Ratio Perturbations, *Proceedings of the 21st International Congress on Sound and Vibration*, Beijing, China, 13–17 July, (2014).

8. Tay-Wo-Chong, L., Bomberg, S., Ulhaq, A., Komarek, T., Polifke, W. Comparative Validation Study on Identification of Premixed Flame Transfer Function, *ASME paper GT2011-46342*.

9. Poinsot T., Veynante, D., *Theoretical and Numerical Combustion, II Edition*, R.T. Edwards, Inc., (2005).

10. Menter, F. R., *Two-Equation Eddy-Viscosity Turbulence Models for Engineering Applications*, AIAA Journal, **32** (8), 1598-1605, (1994).

11. OpenFOAM User Guide. Version 2.3.0, 5 February, (2014).

12. Lipatnikov, A.N., Chomiak, J., Turbulent flame speed and thickness: phenomenology, evaluation, and application in multi-dimensional simulations, *Progress in Energy and Combustion Science*, **28**, 1–74, (2002).

13. Komarek, T., and Polifke, W. Impact of Swirl Fluctuations on the Flame Response of a Perfectly Premixed Swirl Burner, *J. Eng. Gas Turbines Power*, **132**, p. 061503-1,7, (2010).

14. Yasari, E., Verma, S., and Lipatnikov, A.N., RANS simulations of statistically stationary premixed turbulent combustion using Flame Speed Closure model, *Flow, Turb. and Comb.*, **94**: pp. 381-414, (2015).